J Mater Sci: Mater Electron (2022) 33:13782–13791

Studies on modulated physical and photoelectrochemical properties of CdSe thin films by means of Indium doping

V. S. Raut[1], C. D. Lokhande[2], H. D. Shelke[2], and V. V. Killedar[3,*]

[1] Department of Physics, Balwant College Vita (Affiliated to Shivaji University, Kolhapur), Vita 415311, Maharashtra, India
[2] Centre for Interdisciplinary Research, D. Y. Patil University, Kolhapur 416006, Maharashtra, India
[3] Department of Physics, Rajarshi Chhatrapati Shahu College, Kolhapur 416003, Maharashtra, India

Received: 24 October 2021
Accepted: 21 April 2022
Published online: 27 May 2022

ABSTRACT

Well-packed pristine CdSe and Indium-doped CdSe (In:CdSe) thin films have been successfully synthesized on a cost-effective stainless steel substrates by simple chemical route and their performance as photoanode in photoelectrochemical (PEC) solar cell was investigated. With the view to enhance the efficiency of solar cell, various preparative parameters were optimized using renowned PEC way. The Pristine CdSe and In:CdSe thin films were characterized for structural, morphological, optical, and photoelectrochemical studies. The structural analysis revealed modest improvement in crystallinity owed to Indium doping. Morphological modulation noticed from cauliflower structure to elliptical-shaped elongated grains, subsequent to insertion of Indium in CdSe lattice. Doped CdSe photoanodes were found to be more hydrophilic in nature than pristine. Both films possess direct transitions with decrease in band gap energies from 2.1 to 1.91 eV, attributable to doping. Improved power conversion efficiency from 0.54 to 0.79% is recorded as an outcome of indium doping.

1 Introduction

Since earlier few decades, binary semiconductors have captivated a grand extent of notice, owing to several remarkable applications. To triumph over the enduring energy crisis problem, photovoltaic devices are competent for solar to electrical energy conversion, with aid of p–n junctions. In solar cells, the semiconductor–liquid (S–L) junction units are superior over p–n junction unit in view of its built-in storage ability and effortlessness in junction formation [1].

A right and proper choice of photoelectrode material is the prime necessity of proficient solar cell. In this sight, II–VI binary semiconductors are leading contestants. In order to facilitate the progress in PEC solar cells, extensive study of II–VI group binary semiconductors have been undertaken by the researchers, consequent to superior harnessing of solar energy [2]. Among II–VI group semiconductors,

Address correspondence to E-mail: rcsc.physics@gmail.com

https://doi.org/10.1007/s10854-022-08310-w

Cadmium selenide (CdSe) is one of promising candidate that fascinated global researchers because of its suitable properties as size reliant physical and chemical properties, high coefficient of absorption, direct band gap material, luminous properties, etc. Band gap energy of CdSe (Eg = 1.7eV) lies in the vicinity of solar spectrum maxima, hence is most suitable candidate for various optoelectronic applications especially as PEC solar cells [3]. Thus CdSe has been selected as photoanode material for current study.

Doping is one of the ways to transform the physical properties of semiconductors [4–6]. The performance of solar cell can be enhanced by doping photoanode material with suitable dopant. Sahebi et al. [7] have grown CdSe thin film by thermal evaporation method and reported enhanced photovoltaic efficiency as a result of Ag doping in it. Yadav [8] synthesized Fe-doped CdSe thin film by spray pyrolysis technique. He reported highest solar cell efficiency, increased crystallite size, and decreased resistivity and band gap energy subsequent to 0.30 mol.% Fe doping. Shinde et al. [9] electrosynthesized Mn-doped CdSe thin films. They reported improved photoconversion efficiency at the level of 3%Mn doping in CdSe. Rajpure et al. [9] electrodeposited Cd–Fe–Se thin films of different compositions and reported photoconversion efficiency 0.41% and fill factor 50% for 9:1:10 composition. Yadav [10] deposited indium-doped CdSSe thin films by spray pyrolysis and reported improvement in power conversion efficiency from 0.79 to 2.12% as an effect of 0.15 mol.% indium doping. Hankare et al. [11] reported synthesis of indium-doped $Cd_{0.9}Zn_{0.1}Se$ thin films by Chemical bath deposition method. They found maximum photoconversion efficiency of 0.76% concern to 0.1 mol.% indium doping. As doping with indium found to show significant enhancement in performance of PEC cell by decreasing the band gap and enhancing the electrical conductivity of photoelectrode material, thus, in the current study, indium has been chosen as a dopant in the preparation of CdSe photoanode.

Researchers employed diverse physical and chemical methods to synthesize CdSe thin films. Chaudhari et al. [12] prepared CdSe thin films using SILAR method. They explored the correlation between number of immersion cycles and various physical properties. Laatar et al. [14] reported chemosynthesis of CdSe thin films. They reported effect of bath temperature on physical properties of CdSe QD thin films. Swaminathan and Murali [13] reported pulse reversal deposition of CdSe thin films. R. Choudhary and R. P. Chavan [14] synthesized CdSe thin film on glass substrate by spin coating method. They reported effect of gamma irradiations on structural, optical, and morphological properties. Our previous studies [3, 15] report synthesis of pristine CdSe and Indium-doped CdSe thin films using electrodeposition method. In electrodeposition, using pricy potentiostat, it was possible to deposit only single substrate at a time. To overcome this restriction, we contemplated various methods. Comparing to other chemical deposition methods, CBD is an easy and cheap method for the deposition of semiconductor thin films. Using CBD method, with suitably designed holder, it is possible to deposit more number of substrates in single turn. So, for the present study chemical bath deposition (CBD) method has been preferred, on account of several benefits [16–18], such as simplicity in design, high reproducibility, and low cost.

In the present study efforts have been made to deposit pristine CdSe and indium-doped CdSe thin films (In:CdSe) thin films on several substrates in a single turn by low-cost CBD method. Further the outcome of indium doping on structural, morphological, optical, and photoelectrochemical properties is evaluated.

2 Experimental details

2.1 Deposition of CdSe and In:CdSe thin films

2.1.1 *Materials*

All chemicals utilized were of analytical reagent grade (impurity of order of 10^{-3}%) and employed with no extra refinement. For deposition of CdSe thin films, Cadmium sulfate ($CdSO_4.8H_2O$) was used as Cadmium precursor, newly prepared sodium selenosulfate (Na_2SeSO_3) was used as selenium precursor, and 30 vol.% ammonium hydroxide (NH_4OH) was used to regulate pH of chemical bath. Selenium (Se) powder and Sodium sulfate (Na_2SO_3) were used for preparation of Sodium selenosulfate; concern procedure was reported earlier [19]. Stainless steel strips and fluorine-doped tin oxide (FTO)-

coated glass microslides (sheet resistance of 15–20 Ω cm^{-2}) were used as substrates after proper cleaning prior to deposition. For deposition of doped In:CdSe thin films an indium trichloride ($InCl_3$) was used as source material.

2.1.2 *Experimental setup and assembly of PEC cell*

Figure 1 depicts the schematic of experimental setup used for CBD purpose. For the purpose to prepare best photosensitive anode material, use of an illustrious PEC method is made for optimization of synthesis parameters. PEC method involves testing of short-circuit current and open-circuit voltage, i.e., photosensitivity of samples, to decide superior photosensitive sample [20]. Thus, two electrode configuration PEC cell was made, with graphite as counter electrode, CdSe or In:CdSe as photoanode, and 1 M polysulfide as redox electrolyte. Illumination intensity of 50 mW/cm^2 was used to study the PEC cell performance. The exposure photoanode area was 1 cm^2, and residual was covered with insulating tape to avert any other contribution to photocurrent. A PEC solar cell was made in a sealed system by simply direct dipping the photoanode in redox electrolyte.

2.1.3 *Deposition of pristine and doped CdSe thin films*

For chemosynthesis of pristine CdSe thin films, initially 10 ml solution of 0.05 M $CdSO_4$ was poured in a beaker of 30 ml capacity and then under continuous stirring condition liquor ammonia was dropwise added to it. It results in formation of milky cadmium hydroxide $Cd(OH)_2$ precipitate that dissolves subsequent to extra addition of ammonia solution. pH of aqueous bat was maintained to 12 ± 0.2. Lastly 10 ml solution of 0.05 M Na_2SeSO_3 was poured to it. Two substrates are placed 15–20 degrees tilted to wall of beaker. One can also attach minimum eight substrates to substrate holder with beaker of more solution capacity. In order to deposit thin films the beakers were kept in constant temperature bath, whose temperature is then allowed to increase to 85°C and maintained same until deposition process completed. After 8 h, substrates were taken out from reaction bath, dipped carefully in doubly distilled water, dried out at room temperature, and stocked up in airtight container for further characterizations. In a single deposition turn, it is observed that multiple substrates can be easily layered by CBD method carried out using constant temperature water bath.

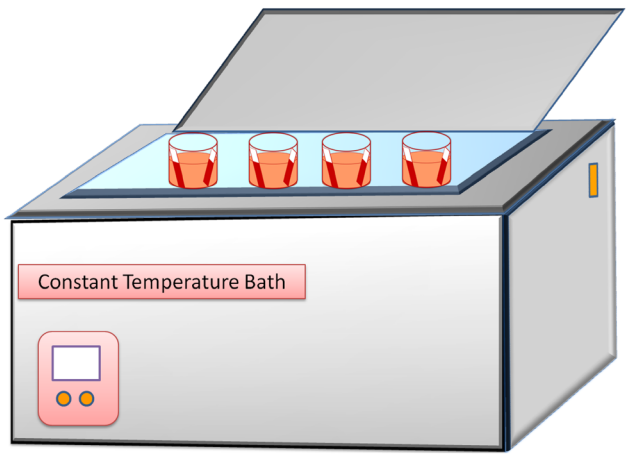

Fig. 1 Schematic of experimental setup used for CBD method

Deposition of Indium-doped CdSe thin film was carried out employing volumetric way of doping with same values of synthesis parameters. Initially solutions for various doping percentages of indium were made. The doping percentage of indium was varied volumetrically for 0.050, 0.1, 0.15, 0.2, 0.25, and 0.5 vol.%. For indium doping percentage higher than 0.5 vol.%, deposition bath becomes milky and turbid. Precipitate of undissolved indium settle down in bath which restricts film formation. Thus doping with indium for higher doping percentage found to be quite problematic.

For deposition of In:CdSe thin films, 10 ml of 0.05 M $CdSO_4$ was taken in a beaker of 30 ml capacity. The accurate volume of indium precursor (0.05 M $InCl_3$) was poured to bath using micropipette so as to maintain volumetric doping percentage for 0.05, 0.1, 0.15, 0.2, 0.25, and 0.5 vol.%. Liquor ammonia was added drop by drop under constant stirring. Ammonia addition to aqueous cadmium precursor results in the formation of milky precipitate of cadmium hydroxide $Cd(OH)_2$, which completely disappears upon further addition of ammonia. Lastly, 10 ml of freshly prepared 0.05 M Na_2SeSO_3 solution was poured to this mixture. Then same procedure repeated as that for deposition of CdSe. Stocked In:CdSe thin films were used for further characterizations.

In order to optimize the doping percentage of indium, PEC method is used. Figure 2 depicts the variation in J_{sc} and V_{oc} with indium volumetric doping percentage. It shows that J_{sc} and V_{oc} increases with increase in indium doping percentage, reaches to maximum values corresponding to 0.2 vol.%

doping percentage, and then drop off for further increase in indium doping percentage. The optimized doping percentage of indium in CdSe thin film was found to be 0.2 vol.%.

Both pristine and 0.2 vol.% In:CdSe thin films were prepared using same optimized preparative parameters and used for further inspections.

2.2 Characterizations

Various characterizations were undertaken for pristine and 0.2 vol.% In:CdSe thin films. The structural study was carried out using Philips X-ray diffractometer varying angle 2θ in range 10–100 degrees. The morphological and compositional studies of thin films were carried out by JEOL-JSM 6360 unit. The optical studies were conducted with a UV spectrophotometer in a wavelength range 300–900 nm. The thickness of both doped and undoped CdSe samples was measured with Ambios XP-1 surface profiler. Wettability studies conducted by means of contact angle measurement using Rame-Hart USA equipment equipped with a CCD camera. Current density–voltage (I–V) characteristics of PEC cell are recorded with a Princeton Applied Research Potentiostat (273A) with a pristine CdSe or 0.2 vol.% In:CdSe electrode as a working electrode and graphite as a counter electrode.

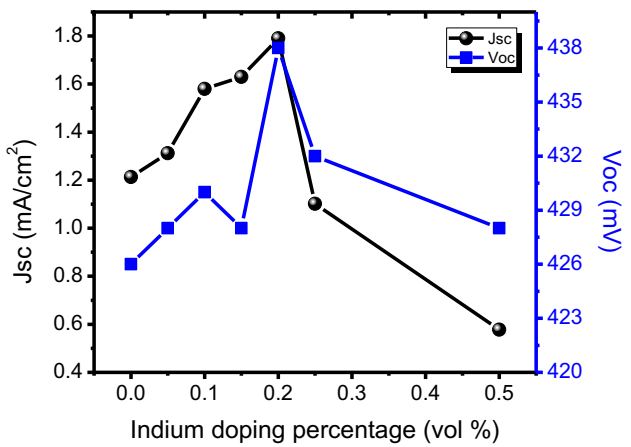

Fig. 2 Variation of J_{sc} and V_{oc} with indium doping percentage

3 Results and discussion

3.1 Structural studies

3.1.1 X-ray diffraction (XRD) studies

Structural properties were studied using distinguished X-ray diffraction (XRD) technique. Figure 3a displays XRD patterns of pristine CdSe and 0.2 vol.% In:CdSe thin films on stainless steel substrate deposited by chemical route. The XRD patterns match well with Standard JCPDS data card no. 00-019-0191 confirming the formation of CdSe with a metastable cubic (Sphalerite) crystal structure. The peaks designated by symbol '*' corresponds to involvement of stainless steel substrate.

The diffraction patterns for pristine and doped CdSe thin films contain five diffraction peaks close to 2θ values 24.3, 25.5, 42.7, 50.5, and 81.8 degrees. The diffraction peaks observed at 25.5, 42.7, 50.5, and 81.8 degrees are indexed as (111), (220), (311), and (511) planes confirming formation of cubic phase which are in good agreement with earlier reports [21, 22]. While the diffraction peak observed close to 2θ value 24.3 degrees is indexed as (100) plane of wurtzite hexagonal phase [JCPDS data card no.00-002-0330] confirming phase change. For doped CdSe thin film trivial enhancement in crystallinity [23] and intensity of hexagonal (100) plane is observed. No any separate peak spotted for indium, CdO, or SeOx.

3.1.2 Raman spectroscopy studies

Figure 3b reveals the Raman spectra of CdSe and 0.2 vol.% In:CdSe thin films deposited by CBD method. The Raman spectrum of CdSe thin film exhibits four peaks with bands at 169.19, 188.10, 208.10, and 235.66 cm^{-1}. The weak band in spectrum at about 208.42 cm^{-1} is ascribed to longitudinal optical (LO) phonon mode of CdSe. The bulk CdSe shows LO phonon mode at 210 cm^{-1} [24]. The red shift observed in LO phonon mode is effect of phonon confinement [25]. The peak observed at around 169.19 cm^{-1} is attributed to transverse optical (TO) phonons. The band at 235.66 cm^{-1} is assigned to out-of-phase Cd–Se–Cd modes [26]. The peak observed at 188.10 cm^{-1} is assigned to surface optical phonon mode. [27].

These bands show shift toward higher frequencies at 170.21, 184.52, 209.78, and 236.38 cm^{-1} for

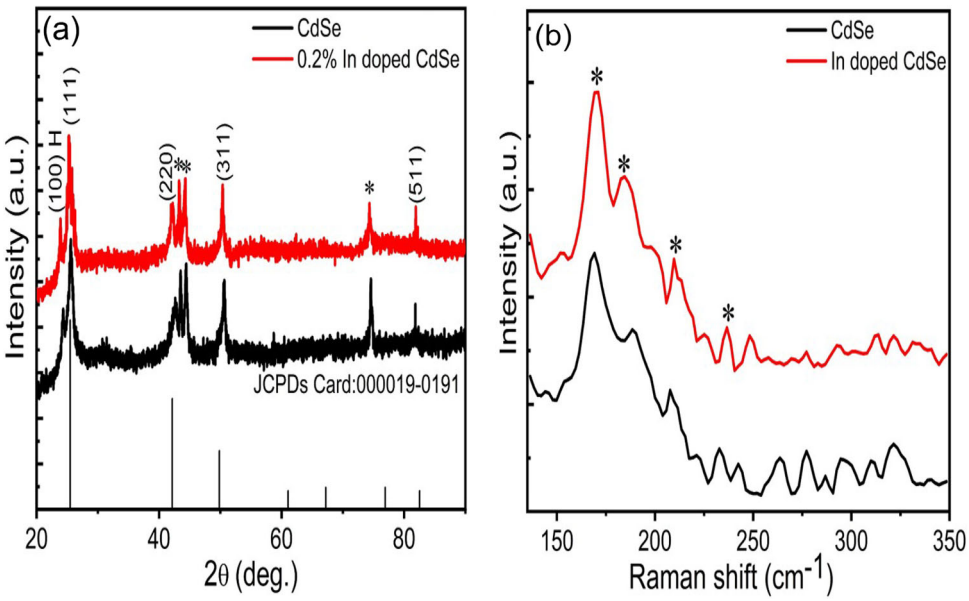

Fig. 3 **a** XRD patterns of chemically synthesized pristine CdSe and In:CdSe thin films. Vertical lines at bottom show standard JCPDS peaks of a cubic phase. **b** Raman spectra of Pristine and 0.2 vol.% doped In:CdSe thin films at room temperature. Symbol * indicates peak position

0.2 vol.% In:CdSe thin film attributed to decrease in bond length due to incorporation of indium ions in CdSe lattice. The Raman shift values for CdSe and 0.2 vol.% In:Cdse thin films are listed in Table 1.

3.2 Surface morphological and compositional studies

The FESEM images of pristine CdSe and 0.2 vol.% In:CdSe thin films at different magnifications as 5 KX and 10 KX are displayed in Fig. 4. Pristine CdSe sample shows compact cauliflower morphology. Cauliflowers of size 2–4 μ are found to be grown all over the substrate. Cauliflower-like structure may get produced as a result of agglomeration and coalescence of small spherical grains. The lower and higher magnification FESEM image of pristine CdSe sample is revealed in Fig. 4a and b, respectively. Kong et al. [28] reported akin morphology for copper thin films grown by electroless deposition. Indium incorporation exhibits considerable variation in morphology. The lower and higher magnification FESEM images of 0.2 vol.% In:CdSe thin film are shown in Fig. 4c and d, respectively. FESEM image of 0.2 vol.% In:CdSe sample clearly shows a compact coating of elliptical-shaped elongated grains.

The composition study to attest presence of indium was conducted using EDAX. Figure 4e shows presence of Cd and Se in CdSe thin film, while Fig. 4f clearly attests the presence of indium along with Cd and Se in a doped sample. The atomic percentage analysis for pristine and doped CdSe thin films is provided in Table 2.

3.3 Optical absorbance and band gap studies

For estimation of band gap energy, the optical absorption study was recorded. Figure 5 shows the plots of $(\alpha h\nu)^2$ against $h\nu$ for pristine and doped CdSe thin film with optical absorption spectra displayed in inset. The linear nature of $(\alpha h\nu)^2$ against $h\nu$ plots

Table 1 Raman shift values for CdSe and 0.2 vol.% In:CdSe thin films

Sample	Pristine CdSe Position (cm^{-1})	0.2 vol.% In:CdSe Position (cm^{-1})
Modes		
Transverse optical	169.19	170.21
Surface optical	188.10	184.52
Longitudinal optical	208.10	209.78
Cd–Se–Cd	235.66	236.38

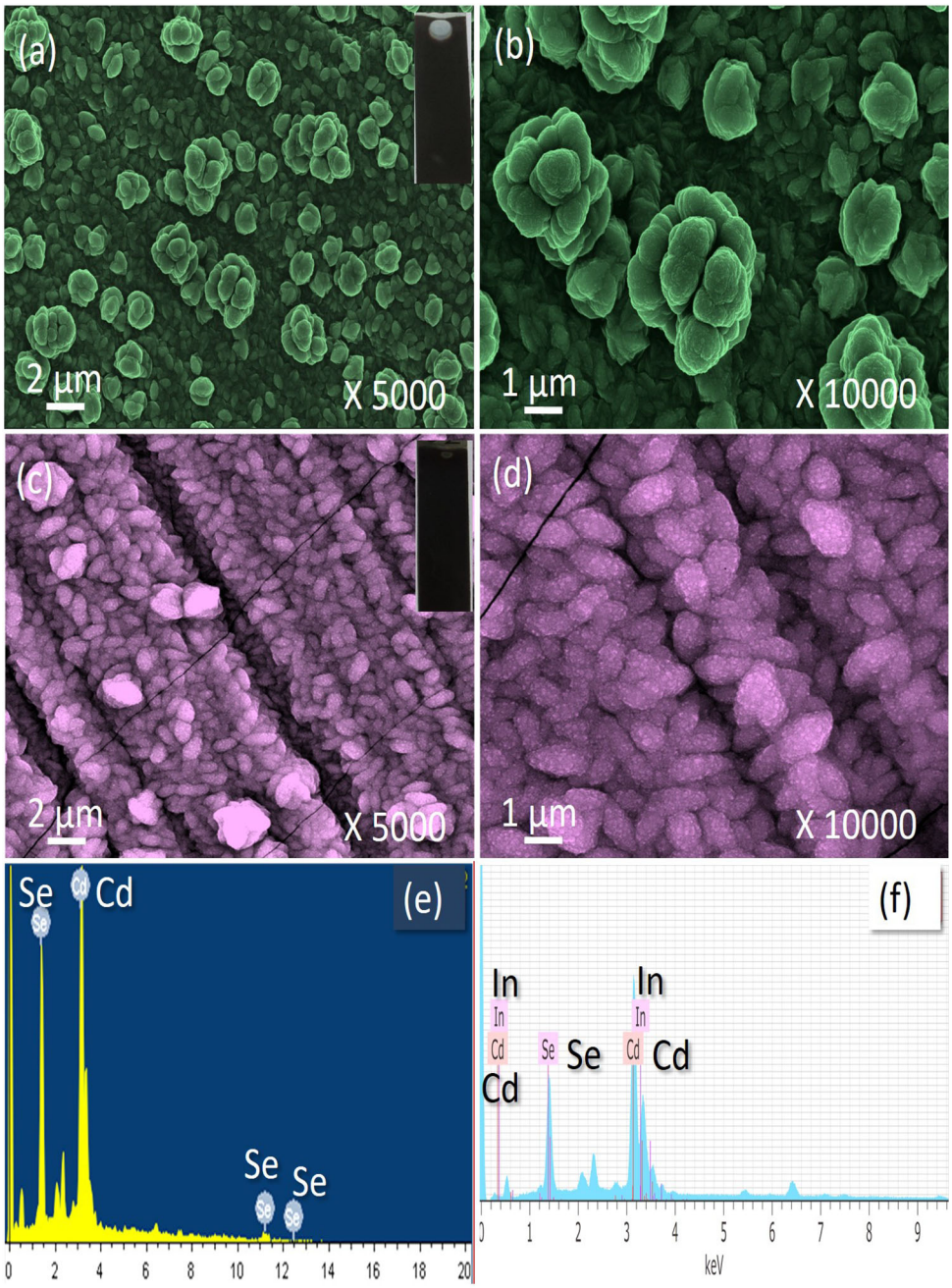

Fig. 4 FESEM images of pristine CdSe (designated as (a), (b)), 0.2 vol.% In:CdSe (designated as (c), (d)) thin films at lower and higher magnification and EDAX patterns of pristine CdSe (e) and 0.2 vol.% In:CdSe sample (f)

Table 2 Compositional particulars of CdSe and In:CdSe samples

Sample	Atomic percentage of the constituent elements		
	Cd	Se	In
Pristine CdSe	62.91	37.09	–
0.2 vol.% In:CdSe	59.99	38.05	1.96

specifies presence of direct transition for both pristine and doped CdSe semiconductors.

The estimated band gap energy for pristine CdSe photoanode is 2.18 eV. After doping, it is found to be decreased to a value 1.91 eV corresponding to

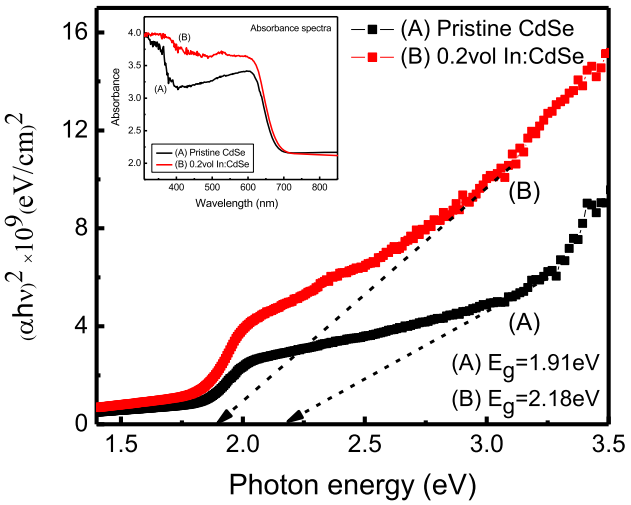

Fig. 5 Band gap plots of pristine CdSe and 0.2 vol.% In:CdSe samples. Inset shows absorbance spectra

indium doping percentage 0.2 vol.%. This may be due to creation of indium donor levels near conduction band in the band gap region due to incorporation of trivalent indium in CdSe matrix [29, 30]. Little red shift is noticed in absorbance spectra of doped thin film than pristine CdSe film. This result can be explained as doping of trivalent indium in CdSe creates indium donor levels in band gap region. This decreases band gap energy, allowing absorption of longer wavelength photons. Band gap reduction in doped thin film shifts absorption edge to longer wavelength side increasing optical absorbance.

3.4 Thickness measurement and surface wettability studies

Variation in film thickness with incorporation of indium in CdSe thin film is displayed in Fig. 6a. Film thickness of doped sample (t = 1212 nm) is found to be slightly greater than pure CdSe sample (1132 nm). Increased film thickness may be one of the reasons for enhanced PEC performance of doped thin film. It can be explained as increase in film thickness increases the light harvesting efficiency resulting in enhanced PEC performance [31].

Figure 6b shows the water contact angle measurement images for pristine CdSe and 0.2 vol.% In:CdSe thin films. The water contact angle values found to be decreased from 73.5 to 58.8 degrees upon indium doping. Scales like structure present on elliptical-shaped elongated grains increases the surface roughness of In:CdSe thin film. It may be responsible for decrease in contact angle upon indium doping. This decrease in water contact angle after doping results in increased hydrophilic nature of electrode surface, which is accountable for improved PEC cell performance [32].

3.5 Photoelectrochemical cell (PEC) analysis

Figure 7 shows the J–V characteristics in dark and under illumination conditions for pristine CdSe and 0.2 vol.% In:CdSe thin films. The current density–voltage (J–V) curves were recorded in dark and under illumination. The PEC cell shows very small current and voltage values in dark condition. The polarity of this current and voltage was found to be negative with respect to CdSe and 0.2 vol.% In:CdSe photoanode. The source of this voltage is accredited to variation in two half-cell potentials of the PEC cell. Under illumination condition, open-circuit voltage increases with negative polarity toward both CdSe and In:CdSe electrodes, signifying that films have n-type conductivity [20].

The values of J_{sc}, V_{oc}, I_m, V_m, FF, η, R_s, and R_{sn} for pristine and 0.2 vol.% In:CdSe samples are listed in Table 3.

For CdSe photoanode, the magnitude of J_{sc} and V_{oc} observed are 1.21 mA/cm^2 and 432 mV, respectively. As a consequence of indium doping these values are found to be enhanced to 1.79 mA/cm^2 and 464 mV, respectively. Thus PEC cell performance was found to be improved with indium doping. The efficiency and fill factor were modified from 0.54 to 0.79% and 52.3 to 47, respectively, as a consequence of indium doping. Shaikh et al. [33] reported 0.49% photoconversion efficiency for electrodeposited CdSe thin films. Shinde et al. [9] reported improvement in photoconversion efficiency of electrodeposited CdSe thin film from 0.36 to 0.54% subsequent to Mn doping. C. Bhattacharya and J. Datta [34] reported photoconversion efficiency of 0.4% for electrosynthsized Cd–Se–Te thin films. Hankare et al. [35] chemically deposited CdSe thin films and reported fill factor and efficiency of 0.36 and 0.55%, respectively. Hankare et al. [11] reported improvement in photoconversion efficiency of chemically deposited $Cd_{0.9}Zn_{0.1}Se$ thin films from 0.61 to 0.76% as an outcome of indium doping. Hankare et al. [36] reported 0.13% photoconversion efficiency for ZnSe thin films deposited by

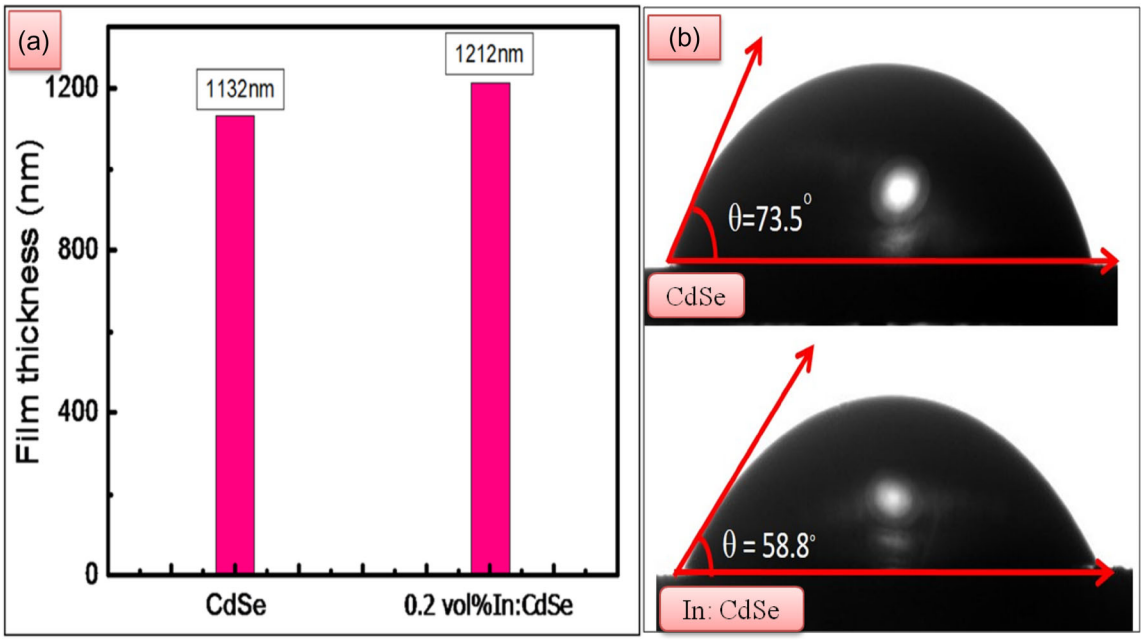

Fig. 6 **a** Film thickness variation for CdSe and In:CdSe thin film. **b** Contact angle images of pristine CdSe and 0.2 vol.% In:CdSe samples

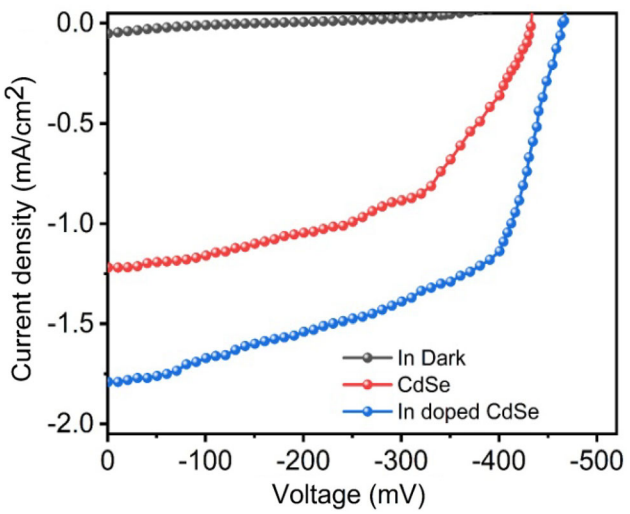

Fig. 7 Power output characteristics of chemically deposited pristine CdSe and 0.2 vol.% In:CdSe /1 M polysulfide/C PEC cells in dark and under illumination

chemical bath deposition method. The photoconversion efficiency of pristine CdSe and indium-doped CdSe thin films reported in our current study is comparatively higher than reported in literature.

The 0.2 vol.% In:CdSe thin film shows superior performance than pure CdSe sample which may be a consequence of creation of In^{3+} donor levels to CdSe lattice in the band gap region. Thus doped indium increases donor concentration causing shift in fermi level position near to the conduction band, resulting in a decreased band gap [37]. Decreased band gap in doped film permits utilization of more portion of the solar energy spectrum, which could be responsible for superior PEC performance of the same. Compared with pristine CdSe photoanode, smaller value of series resistance R_s and larger value of shunt resistance R_{sh} of doped CdSe thin film also turn out well with the performance study.

Table 3 PEC solar cell parameters of chemically deposited pristine CdSe and 0.2 vol.% In:CdSe photoanodes

Parameters	J_{sc} (mA/cm^2)	V_{oc} (mV)	I_m (mA/cm^2)	V_m (mV)	Fill factor	Efficiency (%)	Rs (Ω)	Rsh (Ω)
Sample								
Pristine CdSe	1.21	432	0.85	320.5	52.3	0.54	106	1201
0.2 vol.% In:CdSe	1.79	464	1.12	352	47	0.79	77	1566

4 Conclusion

The pristine CdSe and Indium-doped CdSe thin films were successfully synthesized using low-cost CBD method. The superior PEC performance is recorded corresponding to indium doping of 0.2 vol.%. Indium doping is found to alter structural, optical, and morphological properties of CdSe thin film. Structural study shows pristine CdSe thin film has dominant cubic and weak hexagonal phase, Modest improvement in crystallinity and intensity of hexagonal (100) plane was found resultant to indium doping. Indium incorporation in CdSe lattice upshots morphological alteration. Indium merger in CdSe photoanode decreased water contact angle from 73.5 to 58.8 degrees. Indium doping decreases band gap energy of pristine CdSe photoanode. Doped CdSe thin film showed better PEC performance than pristine one. In conclusion, Indium doping in CdSe photoanode is favorable for PEC solar cell purpose.

Acknowledgements

One of the authors (VSR) is grateful to UGC, New Delhi for award of teacher fellowship.

Author contribution

All the authors participated sufficiently in the manuscript's concept, design, analysis, writing, or revision. All authors examined, critically revised the manuscript, and then approved the final manuscript.

Funding

There are no known competing financial interests or personal relationships that could have appeared to influence the work reported in this paper.

Data availability

Data will be made available on reasonable request.

Declarations

Conflict of interest The authors do not have any competing interests.

Ethical approval This manuscript is original, has not been published before, and is not currently being considered for publication elsewhere. The paper reflects the authors' own research and analysis in a truthful and complete manner.

References

1. N.M. Shinde, D.P. Dubal, D.S. Dhawale, C.D. Lokhande, J.H. Kim, J.H. Moon, Mater. Res. Bull. **47**, 302 (2012). https://doi.org/10.1016/j.materresbull.2011.11.020
2. C.S. Bagade, V.B. Ghanwat, K.V. Khot, P.N. Bhosale, Mater. Lett. **164**, 52 (2016). https://doi.org/10.1016/j.matlet.2015.10.099
3. V.S. Raut, C.D. Lokhande, V.V. Killedar, J. Mater. Sci. Mater. Electron. **28**, 3140 (2017). https://doi.org/10.1007/s10854-016-5902-6
4. L.N. Maskaeva, V.F. Markov, O.A. Lipina, A.V. Pozdin, I.A. Anokhina, Russ. J. Phys. Chem. **94**, 2441 (2020). https://doi.org/10.1134/S0036024420120195
5. G. Perna, V. Capozzi, A. Minafra, M. Pallara, M. Ambrico, Eur. Phys. J. B **32**, 339 (2003). https://doi.org/10.1140/epjb/e2003-00107-6
6. Q. Dai, E.M. Sabio, W. Wang, J. Tang, Appl. Phys. Lett. **104**(18), 183901 (2014). https://doi.org/10.1063/1.4875107
7. R. Sahebi, M.R. Roknabadi, M. Behdani, Mater. Res. Express. **6**, 126453 (2019). https://doi.org/10.1088/2053-1591/ab6c17
8. A.A. Yadav, J. Alloys Compd. **543**, 129 (2012). https://doi.org/10.1016/j.jallcom.2012.07.097
9. S.K. Shinde, D.P. Dubal, G.S. Ghodake, V.J. Fulari, J. Electroanal. Chem. **727**, 179 (2014). https://doi.org/10.1016/j.jelechem.2014.04.005
10. K.Y. Rajpure, P.A. Anarase, C.D. Lokhande, C.H. Bhosale, Phys. Stat. Sol. (a) **172**(2), 415 (1999)
11. A.A. Yadav, J. Mater. Sci. Mater. Electron. **27**, 4508 (2016). https://doi.org/10.1007/s10854-016-4325-8
12. P.P. Hankare, P.A. Chate, D.J. Sathe, Phys. B **404**, 2389 (2009). https://doi.org/10.1016/j.physb.2009.04.048
13. K.B. Chaudhari, N.M. Gosavi, N.G. Deshpande, S.R. Gosavi, J. Sci.: Adv. Mater. Dev. **1**, 476 (2016). https://doi.org/10.1016/j.jsamd.2016.11.001
14. F. Laatar, A. Harizi, A. Smida, M. Hassen, H. Ezzaouia, Mater. Res. Bull. **78**, 83 (2016). https://doi.org/10.1016/j.materresbull.2016.02.021
15. V. Swaminathan, K.R. Murali, Sol. Energy Mater. Sol. Cells. **63**(2), 207 (2000). https://doi.org/10.1016/S0927-0248(00)00010-6

16. R. Choudhary, R.P. Chavan, J. Mater. Sci. Mater. Electron. **27**, 11674 (2016). https://doi.org/10.1007/s10854-016-5303-x
17. V.S. Raut, C.D. Lokhande, V.V. Killedar, J. Electroanal. Chem. **788**, 137–143 (2017). https://doi.org/10.1016/j.jelechem.2017.02.010
18. G. Hodes, Phys. Chem. Chem. Phys. **9**(18), 2181 (2007). https://doi.org/10.1039/B616684A
19. G.H. Fekadu, A. Tizazu, Int. J. Thin. Fil. Sci. Tec. **8**(2), 43 (2019). https://doi.org/10.18576/ijtfst/080203
20. S.M. Ho, Res. J. Appl. Sci. Eng. Tech. **11**(10), 1058 (2015). https://doi.org/10.19026/rjaset.11.2119
21. V.S. Raut, V.V. Killedar, C.D. Lokhande, Int. J. Eng. Res. Technol. **10**(1), 568 (2017)
22. S.M. Pawar, A.V. Moholkar, K.Y. Rajpure, C.H. Bhosale, J. Phys. Chem. Solids **10**(1), 2386 (2006). https://doi.org/10.1016/j.jpcs.2006.06.015
23. H. Sabri, S. Saleh, A. Zyoud, N.N. Abdel-Rahman, I. Saadeddin, G. Campet, D. Park, M. Faroun, H.S. Hilal, Electrochim. Acta. **136**, 138 (2014). https://doi.org/10.1016/j.electacta.2014.05.071
24. M. Piryaei, E.G. Hatam, N. Ghobadi, J. Mater. Sci. Mater. Electron. **28**, 2550 (2017). https://doi.org/10.1007/s10854-016-5830-5
25. G.S. Shahane, K.M. Garadkar, L.P. Deshmukh, Mater. Chem. Phys. **51**, 246 (1997). https://doi.org/10.1016/S0254-0584(97)80313-6
26. E.C.F. da Silva and D. Strauch, Landolt-Börnstein—Group III Condensed Matter Volume 44E, New Data and Updates for several III–V (including mixed crystals) and II–VI Compounds. DOI: https://doi.org/10.1007/978-3-642-23415-6_77 (Springer-Verlag Berlin Heidelberg 2012) p. 134.
27. V.M. Dzhagan, M.Y. Valakh, A.E. Raevskaya, A.L. Stroyuk, S.Y. Kuchmiy, D.R.T. Zahn, Nanotechnology **19**, 305707 (2008). https://doi.org/10.1088/0957-4484/19/30/305707
28. S. Das, A. Dutta, S. Banerjee, T.P. Sinha, Mater. Sci. Semicond. Process. **18**, 152 (2014). https://doi.org/10.1016/j.mssp.2013.11.023
29. S. Wageh, Physica E **39**, 8 (2007). https://doi.org/10.1016/j.mssp.2013.11.023
30. C. Kong, S. Sun, J. Zhang, H. Zhao, X. Song, Z. Yang, Cryst. Eng. Comm. **14**, 5737 (2012). https://doi.org/10.1039/C2CE25709B
31. A.A. Yadav, M.A. Barote, T.V. Chavan, E.U. Masumdar, J. Alloys Compd. **509**, 916 (2011). https://doi.org/10.1016/j.jallcom.2010.09.130
32. A.M. Perez Gonalez, I.V. Arreola, REVISTA MEXICANA DE FI´SICA 55, 51 (2009) DESCARGAR ARTÍCULO EN FORMATO PDF
33. J. Xiao, L. Peng, L. Gao, J. Zhong, Z. Huang, E. Yuan, V. Srinivasapriyan, S.F. Zhou, G. Zhan, RSC Adv. **11**, 16600 (2021). https://doi.org/10.1039/d1ra02826j
34. S.K. Shinde, D.P. Dubal, G.S. Ghodake, V.J. Fulari, RSC Adv. **4**, 33184 (2014). https://doi.org/10.1039/C4RA02791D
35. A. V. Shaikh, R.S. Mane, O. S. Joo, B. N. Pawar, J. K. Lee, S. H. Wan Han, J. Phys Chem solids. 72(10), 1122 (2011). DOI :https://doi.org/10.1016/j.jpcs.2011.06.017
36. C. Bhattacharya, J. Datta, J Solid State Electrochem **11**, 215 (2007). https://doi.org/10.1007/s10008-005-0091-x
37. P.P. Hankare, P.A. Chate, D.J. Sathe, M.R. Asabe, B.V. Jadhav, J. Alloys Compd. **474**(1–2), 347 (2009). https://doi.org/10.1016/j.jallcom.2008.06.081
38. P.P. Hankare, P.A. Chate, P.A. Chavan, D.J. Sathe, J. Alloys Compd. **461**, 623 (2008). https://doi.org/10.1016/j.jallcom.2007.07.071
39. S.J. Lade, M.D. Uplane, C.D. Lokhande, Mater. Chem. Phys. **68**, 36 (2001). https://doi.org/10.1016/S0254-0584(00)00280-7

Terms and Conditions

Springer Nature journal content, brought to you courtesy of Springer Nature Customer Service Center GmbH (“Springer Nature”).
Springer Nature supports a reasonable amount of sharing of research papers by authors, subscribers and authorised users (“Users”), for small-scale personal, non-commercial use provided that all copyright, trade and service marks and other proprietary notices are maintained. By accessing, sharing, receiving or otherwise using the Springer Nature journal content you agree to these terms of use (“Terms”). For these purposes, Springer Nature considers academic use (by researchers and students) to be non-commercial.
These Terms are supplementary and will apply in addition to any applicable website terms and conditions, a relevant site licence or a personal subscription. These Terms will prevail over any conflict or ambiguity with regards to the relevant terms, a site licence or a personal subscription (to the extent of the conflict or ambiguity only). For Creative Commons-licensed articles, the terms of the Creative Commons license used will apply.
We collect and use personal data to provide access to the Springer Nature journal content. We may also use these personal data internally within ResearchGate and Springer Nature and as agreed share it, in an anonymised way, for purposes of tracking, analysis and reporting. We will not otherwise disclose your personal data outside the ResearchGate or the Springer Nature group of companies unless we have your permission as detailed in the Privacy Policy.
While Users may use the Springer Nature journal content for small scale, personal non-commercial use, it is important to note that Users may not:

1. use such content for the purpose of providing other users with access on a regular or large scale basis or as a means to circumvent access control;
2. use such content where to do so would be considered a criminal or statutory offence in any jurisdiction, or gives rise to civil liability, or is otherwise unlawful;
3. falsely or misleadingly imply or suggest endorsement, approval , sponsorship, or association unless explicitly agreed to by Springer Nature in writing;
4. use bots or other automated methods to access the content or redirect messages
5. override any security feature or exclusionary protocol; or
6. share the content in order to create substitute for Springer Nature products or services or a systematic database of Springer Nature journal content.

In line with the restriction against commercial use, Springer Nature does not permit the creation of a product or service that creates revenue, royalties, rent or income from our content or its inclusion as part of a paid for service or for other commercial gain. Springer Nature journal content cannot be used for inter-library loans and librarians may not upload Springer Nature journal content on a large scale into their, or any other, institutional repository.
These terms of use are reviewed regularly and may be amended at any time. Springer Nature is not obligated to publish any information or content on this website and may remove it or features or functionality at our sole discretion, at any time with or without notice. Springer Nature may revoke this licence to you at any time and remove access to any copies of the Springer Nature journal content which have been saved.
To the fullest extent permitted by law, Springer Nature makes no warranties, representations or guarantees to Users, either express or implied with respect to the Springer nature journal content and all parties disclaim and waive any implied warranties or warranties imposed by law, including merchantability or fitness for any particular purpose.
Please note that these rights do not automatically extend to content, data or other material published by Springer Nature that may be licensed from third parties.
If you would like to use or distribute our Springer Nature journal content to a wider audience or on a regular basis or in any other manner not expressly permitted by these Terms, please contact Springer Nature at

onlineservice@springernature.com